

Layer-adapted meshes for singularly perturbed problems via mesh partial differential equations and *a posteriori* information

Róisín Hill¹ and Niall Madden²

¹*Department of Mathematics & Statistics, University of Limerick, Ireland. Corresponding author.*

Email: roisin.hill@ul.ie.

²*School of Mathematical and Statistical Sciences, University of Galway, Ireland.*

Email: Niall.Madden@UniversityofGalway.ie

November 3, 2023

Abstract

We propose a new method for the construction of layer-adapted meshes for singularly perturbed differential equations (SPDEs), based on mesh partial differential equations (MPDEs) that incorporate *a posteriori* solution information. There are numerous studies on the development of parameter robust numerical methods for SPDEs that depend on the layer-adapted mesh of Bakhvalov. In (Hill and Madden, 2021), a novel MPDE-based approach for constructing a generalisation of these meshes was proposed. Like with most layer-adapted mesh methods, the algorithms in that article depended on detailed derivations of *a priori* bounds on the SPDE's solution and its derivatives. In this work we extend that approach so that it instead uses *a posteriori* computed estimates of the solution. We present detailed algorithms for the efficient implementation of the method, and numerical results for the robust solution of two-parameter reaction-convection-diffusion problems, in one and two dimensions. We also provide full FEniCS code for a one-dimensional example.

Key words: Mesh PDEs, finite element methods, PDEs, singularly-perturbed, layer-adapted meshes.
AMS subject classification: 65N50, 65N30, 65-04

1 Introduction

This article is concerned with a new approach to generating layer-adapted meshes for singularly perturbed differential equations (SPDEs). The core idea is to use a new formulation for the classic fitted meshes of Bakhvalov (Bakhvalov, 1969) proposed in (Hill and Madden, 2021), but extended to use *a posteriori* computed quantities, rather than the usual *a priori* information usually used to construct these meshes.

For exposition, we will focus on the numerical solution of two-parameter reaction-convection-diffusion equations of the form

$$-\varepsilon\Delta u(x) + \mu\mathbf{b} \cdot \nabla u(x) + r(x)u(x) = f(x) \quad \text{for } x \in \Omega^d, \quad \text{with } u|_{\partial\Omega} = 0, \quad (1)$$

with $d = 1, 2$. We make rather standard assumptions on the other problem data; specifically that \mathbf{b} , r , and f are given smooth functions, and that $2r > \mu \operatorname{div} \mathbf{b}$. Equation (1) features a pair of positive parameters, ε and μ , which may be arbitrarily small, making this a *singularly perturbed* problem. Typically, solutions to (1) exhibit layers, the location and width of which can be challenging to determine *a priori* (especially when $d = 2$), making it particularly interesting for exhibiting the features of our proposed method. The proposed method automatically determines these quantities, and constructs an appropriate mesh by solving a suitable mesh partial differential equation (MPDE). This is done in practice by alternating between solving the SPDE and the MPDE on a nested sequence of grids using standard Galerkin finite element methods.

SPDEs, such as (1), are of interest to mathematical modellers, since they can be applied to describe a wide range of physical phenomena. Their numerical solution is of significant interest in numerical

analysis, and great efforts have been made to devise (and analyse) methods which can solve such problems accurately, and resolve any layers present. A detailed overview of the field (as it was in 2008) is given in (Roos et al., 2008); see also (Roos, 2022) for a more recent view of advances and challenges.

One of the challenges in the numerical solution of singularly perturbed problems is the development of methods for which a meaningful error bound can be established that is independent of the perturbation parameter(s), and which ensure any layers present are resolved; the monograph of (Miller et al., 2012) provide detailed motivation for this and presents methods that enjoy these properties, for a wide class of problems. These methods are mainly based on the famous piecewise uniform Shishkin mesh (Shishkin and Shishkina, 2009). We refer to (Linß, 2010) for a more general treatment, which includes analyses for other meshes, including the graded Bakhvalov mesh (Bakhvalov, 1969).

The meshes mentioned above are constructed based on *a priori* information on the solution and its derivatives. The approach that we present is closer in philosophy to *a posteriori* adaptive algorithms, of which there are many in the literature; notable examples include the now-classic work of Beckett and Mackenzie (2000) and Kopteva and Stynes (2001). We also mention Sikwila and Shateyi (2013); Shakti et al. (2022), which are closer in style to this article, since they use moving mesh methods, as well as the work on reaction-convection-diffusion problems of Wu et al. (2013). However, the method that we propose is distinguished in that our goal is to automatically reconstruct the mesh density function of a Bakhvalov mesh, rather than by adapting the mesh directly.

We emphasise that our goal is not to present an algorithm for (1), *per se*, but to use it as a test case for testing our approach. Furthermore, since the details of the construction of the usual Bakhvalov mesh may differ substantially from when $d = 1$ to $d = 2$, we defer a detailed description (and review of the literature) to §2.1 and §3.1, respectively.

The rest of this article is organised as follows. In the next section, we summarise some notation used throughout. We then turn our attention to one-dimensional versions of (1) in §2. The background and some key references are discussed in §2.1 In §2.2 we present the MPDE that we use to generate the meshes on which to solve the SPDE. We present the algorithm to generate these meshes and detail how our method is implemented in §2.3. In §2.4 we present the results of numerical experiments which verify the accuracy and efficiency of the method.

In §3 we extend the approach to two-dimensional reaction-convection-diffusion problems, where, in addition to the relationship between the two parameters, the direction of the flow influences the nature and location of layers. We present the MPDE formulations in §3.2, and the implementation in §3.3. Again, validating numerical results are presented in §3.4. We use a standard Galerkin \mathcal{P}_1 finite element method to solve both the MPDEs and SPDEs. All results presented have been computed using FEniCS (Logg et al., 2012), with a full working example presented in Appendix A. We present pseudo-code for the two-dimensional problem in Appendix B.

Notation and definitions

We use Ω to denote an open, bounded subset of \mathbb{R}^d , $\bar{\Omega}$ denotes its closure, and $\partial\Omega$ its boundary. Usually, it is the domain on which a (physical) SPDE is posed. We denote the computational domain (on which the MPDE is posed) as $\Omega^{[c]}$.

Where necessary, we use a superscript to indicate a differential operator applied on the computational domain. In particular, we define

$$\nabla^{[c]} = \left(\frac{\partial}{\partial \xi_1}, \frac{\partial}{\partial \xi_2} \right), \quad \text{for } (\xi_1, \xi_2) \in \Omega^{[c]}.$$

We use ω_h to denote a mesh that discretizes $\bar{\Omega}$, and $\omega_h^{[c]}$ as a mesh on $\Omega^{[c]}$. That is, it denotes a partition, for the purposes of finite element discretization, into simplices of $\bar{\Omega}$, i.e., intervals in one dimension and triangles in two dimensions. In addition, $\omega_h^{[c]}$ denotes a partition of a computational domain, $\bar{\Omega}^{[c]}$. A member of a sequence of partitions of $\bar{\Omega}$ or of $\bar{\Omega}^{[c]}$ is denoted $\omega_h^{[i]}$ or $\omega_h^{[c,i]}$.

Definition 1.1 (The one-dimensional equidistribution principle). Let $\rho := \bar{\Omega} \rightarrow \mathbb{R}_{>0}$ be a strictly positive function known as the *mesh density function*. We say that the mesh $\omega_h := \{a = x_0 < x_1 < \dots < x_{N-1} < x_N = b\}$ *equidistributes* ρ , if

$$\int_{x_{i-1}}^{x_i} \rho(x) dx = \frac{1}{N} \int_{\bar{\Omega}} \rho(x) dx \quad \text{for } i = 1, \dots, N.$$

Definition 1.2 (Mesh generating function). A mesh generating function is a strictly monotonic bijective function $\varphi : \bar{\Omega}^{[cl]} := [0, 1] \rightarrow \bar{\Omega} := [a, b]$ that maps a uniform mesh with mesh points $\xi_i = i/N$, for $i = 0, 1, \dots, N$, to a (possibly non-uniform) mesh with mesh points $x_i = \varphi(i/N)$, for $i = 0, 1, \dots, N$, with $\varphi(0) = a$ and $\varphi(1) = b$.

2 One-dimensional problems

2.1 A one-dimensional SPDE

In this section, we focus on the generation of meshes for solving the one-dimensional reaction-convection-diffusion problem

$$-\varepsilon u''(x) + \mu b(x)u'(x) + r(x)u(x) = f(x) \quad \text{for } x \in (0, 1), \quad \text{and } u(0) = u(1) = 0. \quad (2)$$

When ε is small, and μ is $\mathcal{O}(1)$ and positive, and assuming that f does not vanish at either boundary, a layer of width $\mathcal{O}(\varepsilon)$ will typically form on the right of the domain. If μ is negative, the layer would be manifested near the left boundary. However, if $\mu \ll 1$, which makes this a so-called ‘‘two-parameter’’ problem, then the situation is more complicated, and there may be layers at both boundaries, whose widths depend on the relative magnitude of ε and μ .

In spite of their apparent simplicity, one-dimensional linear problems such as (2) are widely studied (since, at least, the work of (O’Malley, 1967)). In the numerical analysis literature, progress was made in the early 2000s (see, e.g., (Roos and Uzelac, 2003; Gracia et al., 2006)). Research into these problems continues; see, e.g., the analyses of a discontinuous Galerkin method on *a priori* layer-adapted meshes (Singh and Natesan, 2020), and an investigation of uniform convergence and supercloseness for the \mathcal{P}_1 -FEM solution on a graded meshes (Zhang and Lv, 2022).

Of particular interest to us is the analysis of a continuous Galerkin FEM applied on a Bakhvalov mesh (Brdar and Zarin, 2016). The level of detail in that paper demonstrates the complexity in even constructing a suitable mesh for this problem. The reason for this complexity is due to the interplay between the values of ε and μ which determines the location and width of layers. This complicates the specification of *a priori* layer-adapted meshes, but not for the approach we propose, which automatically generates layer-adapted meshes for this problem without prior knowledge of the relationship between the two-parameters.

We present the general approach (for any one-dimensional problem featuring boundary layers) in §2.2, with more specific details of the algorithm given in §2.3. In §2.4 we show how the approach produces suitable meshes for a challenging two-parameter problem with layers of different widths.

2.2 A one-dimensional MPDE for Bakhvalov meshes

In the literature, there are two distinct (but equivalent) approaches to constructing meshes of Bakhvalov type. The original approach depends on solving a certain non-linear problem (see, e.g., (Linß, 2010, §2.1.1) and (Hill and Madden, 2021, §2.2)). As noted in (Linß, 2010, §6.3), these meshes can also be constructed by equidistributing certain monitor functions. For a problem such as (2), where the solution may have a layer near each of the boundaries, one equidistributes a mesh density function of the form

$$\rho(x) = \max \left\{ 1, K\lambda_0 \exp(-\lambda_0 x \sigma^{-1}) + K\lambda_1 \exp(-\lambda_1 (1-x) \sigma^{-1}) \right\}, \quad (3)$$

where λ_0 and λ_1 are related to the width of the layers, σ is determined by the formal order of the scheme, and $0 < K < 1$ is chosen to control the proportion of the mesh points in the layer regions.

It known that the mesh generating function for a mesh on $\bar{\Omega} := [a, b]$ that equidistributes an arbitrary mesh generating function, ρ , can be expressed as the solution to the mesh PDE

$$(\rho(x)x_\xi(\xi))_\xi = 0, \text{ for } \xi \in \Omega^{[c]} := (0, 1), \text{ with } x(0) = a \text{ and } x(1) = b; \quad (4)$$

see (Hill and Madden, 2021) for details. In the approach in that paper, 4 is solved numerically with a \mathcal{P}_1 -FEM, to obtain a mesh generating function. For the classical construction of a Bakhvalov mesh, ρ depends on *a priori* information concerning the solution of the physical differential equation; in (3) it can be thought of as representing point-wise bounds for $|u'(x)|$.

We now present an alternative approach, where $\rho = \rho(x, u_h)$ is based on derivatives of numerical solutions to the SPDEs. The resulting algorithm anticipates that there may be boundary layers present, but does not require *a priori* knowledge concerning the boundaries at which layers may be present, or of the width of those layers. The MPDE (4) is reformulated as

$$(\rho(x, u_h)x_\xi(\xi))_\xi = 0, \text{ for } \xi \in \Omega^{[c]}, \text{ with } x(0) = 0 \text{ and } x(1) = 1, \quad (5)$$

to emphasise that now ρ is dependent on the numerical solution to the physical differential equation. For (2), we take

$$\rho(x, u_h) = \max \left\{ 1, K(v_0 \exp(-v_0 x \sigma^{-1}) + v_1 \exp(-v_1(1-x)\sigma^{-1})) \right\}, \quad (6a)$$

with

$$v_0(x, u_h) = \frac{|(u_h)_{x^+}(x_0)|}{\max\{1, |f(x_0)|\}} \quad \text{and} \quad v_1(x, u_h) = \frac{|(u_h)_{x^-}(x_N)|}{\max\{1, |f(x_N)|\}}, \quad (6b)$$

where f is the right-hand side of the SPDE. It should be noted that this formulation is independent of the number of boundary layers present in the solution, and their location(s) and width(s). For example, if the solution possesses just one layer near, which is near $x = 1$, then $(u_h)_{x^-}(x_N) \gg 1$ leading to a graded mesh near that boundary; elsewhere one will have $\rho(x, u_h) = 1$, giving a uniform coarse mesh over the rest of the domain.

Remark 1. The term $\max\{1, |f(x_0)|\}$ in (6b) handles the case where, for example, $f(0) = 0$. Note that, in such an instance, the solution to (2) would not exhibit a strong boundary layer near $x = 0$, in the sense that $u'(0)$ would be bounded independently of ε . Higher derivatives of u at $x = 0$ would not be bounded, so some minor modifications of the approach may be need if using, for example, high-order finite elements.

2.3 Algorithm and implementation

In Algorithm 1 we outline a mechanism for solving the nonlinear equation (5) in an efficient manner. At its core is a fixed-point iterative method, but it is accelerated by using h -refinement (Hill and Madden, 2021). The inner iteration involves solving both the SPDE and MPDE, since the latter requires accurate estimates of the derivatives of the solution to the SPDE.

The process begins by solving the SPDE on a uniform mesh with 16 elements (with fewer, a layer cannot be detected even for relatively large values of ε). This is used to compute ρ in (6), and thence a linearisation of (4). This yields a new mesh on which the SPDE can be solved, and this process is iterated until

$$\Delta^{[k]} := \left| \frac{(u_h^{[k]})_{x^+}(x_0) - (u_h^{[k-1]})_{x^+}(x_0)}{(u_h^{[k]})_{x^+}(x_0)} \right| + \left| \frac{(u_h^{[k]})_{x^-}(x_N) - (u_h^{[k-1]})_{x^-}(x_N)}{(u_h^{[k]})_{x^-}(x_N)} \right|,$$

is less than some chosen tolerance. Then the mesh is uniformly refined, and the iterative process repeated, until the computational mesh has the desired number of intervals.

Inputs: N , the number of intervals in the final mesh; ρ , a mesh density function; TOL.

- 1 Set $\omega_h^{[c;0]} := \{\xi_0, \xi_1, \dots, \xi_{16}\}$ to be the uniform mesh on $\overline{\Omega}^{[c]}$ with 16 intervals;
- 2 Set $x(\xi) = \xi$ for $\xi \in \overline{\Omega}^{[c]}$;
- 3 $r \leftarrow x$; $k \leftarrow 0$;
- 4 **for** i in $0:(\log_2(N)-4)$ **do**
- 5 **do**
- 6 Set $\omega_h^{[k]} := x(\omega_h^{[c;i]})$ to be the adapted mesh on $\overline{\Omega}$ at step k ;
- 7 $u_h^{[k]} \leftarrow \mathcal{P}_1$ -FEM solution to the SPDE on $\omega_h^{[k]}$;
- 8 Calculate $\Delta^{[k]}$;
- 9 Calculate $v_l(r, u_h^{[k]})$ for $l = 0, 1$, and then $\rho(r, u_h^{[k]})$;
- 10 set x to be the \mathcal{P}_1 -FEM solution, on $\omega_h^{[c;i]}$, to

$$(\rho(r, u_h^{[k]})x'(\xi))' = 0, \text{ for } \xi \in \Omega^{[c]}, x(0) = a \text{ and } x(1) = b;$$
- $r \leftarrow x$; $k \leftarrow k+1$;
- 11 **while** $\Delta^{[k]} > \text{TOL}$;
- 12 **if** $|\omega_h^{[c;i]}| < N+1$ **then**
- 13 $\omega_h^{[c;i+1]} \leftarrow$ uniform h -refinement of $\omega_h^{[c;i]}$;
- 14 $r \leftarrow r$ interpolated onto $\omega_h^{[c;i+1]}$;
- 15 **end**
- 16 **end**
- 17 Set $\omega_h := x(\omega_h^{[c;i]})$ to be the (final) adapted mesh on $\overline{\Omega}$;

Algorithm 1: Generate a layer-adapted mesh using an MPDE, h -refinement and *a posteriori* information.

2.4 Numerical results

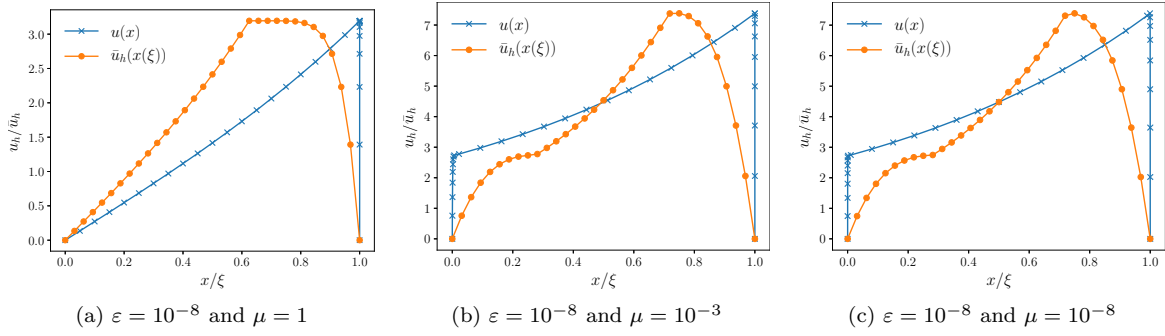
We now consider a specific sets of problems of the form

$$-\varepsilon u''(x) + \mu u'(x) + u(x) = e^{1+x}, \quad \text{for } x \in \Omega := (0, 1), \quad \text{with } u(0) = u(1) = 0, \quad (7)$$

where $0 < \varepsilon \ll 1$ and $0 < \mu \leq 1$. This problem is interesting because the location and width of layers present in solutions depend on the relative magnitude of ε and μ , leading to three distinct regimes, as summarised in Table 1 (see (Linß, 2010, §3.2)). Examples of solutions for each regime on both the physical domain, Ω , and the computational domain, $\Omega^{[c]}$, are shown in Figure 1.

Table 1: Location and width of layers, depending on the magnitude of ε and μ .

Case	Regime	rate of decay is determined by		
		$x = 0$	$x = 1$	
(a)	$\varepsilon \ll \mu = 1$	1	$1/\varepsilon$	(convection-diffusion)
(b)	$\varepsilon \ll \mu^2 \ll 1$	$1/\mu$	μ/ε	(reaction-convection-diffusion)
(c)	$\mu^2 \ll \varepsilon \ll 1$	$1/\sqrt{\varepsilon}$	$1/\sqrt{\varepsilon}$	(reaction-diffusion)

Figure 1: FEM solutions to (7) under each regime with $N = 32$ on Ω and $\Omega^{[c]}$

In (Brdar and Zarin, 2016) it is proven that for one-dimensional reaction-convection-diffusion equations the errors measured in the energy norm are bounded as

$$\|u - u_h\|_{\mathbb{E}} \leq C \left((\varepsilon^{1/2} + \mu)^{1/2} N^{-1} + N^{-2} \right), \quad (8)$$

where u is the exact solution, u_h is the \mathcal{P}_1 -FEM solution to the SPDE, computed on a Bakhvalov-type mesh and

$$\|u\|_{\mathbb{E}} := (\varepsilon \|u'\|_0^2 + \|u\|_0^2)^{1/2}.$$

A Bakhvalov mesh for this problem equidistributes (3) where λ_0 and λ_1 are related to (ordered) solutions of

$$-\varepsilon \lambda(x)^2 + \mu b(x) \lambda(x) + r(x) = 0.$$

To verify that solutions computed on the meshes produced by our algorithm satisfy the same bounds as in (8), we estimate the errors, $\|E_h\|_{\mathbb{E}} := \|u_h - u_{2,h}\|_{\mathbb{E}}$, where $u_{2,h}$ is the \mathcal{P}_2 -FEM solution to the SPDE, computed on the same mesh as u_h .

First, in Table 2, we consider the convergence of the scheme by presenting results over a range of values of N . We have fixed $\mu = 10^{-3}$, and taken various values for ε , so that each of the three regimes is represented. The errors for (7) are reported, along with the rates of convergence. The number of iterations of the MPDE method performed on the final mesh size is shown in parentheses. For these calculations, we have taken $K = 0.28$ (resulting in approximately 30% of mesh points in each layer region) and $\sigma = 2.5$ in (6), and $\text{TOL} = 10^{-3}$ in Algorithm 1. The results show that the method yields a consistently robust order of convergence and that the number of iterations needed on the final mesh is independent of ε and N .

Table 2: $\|E_h\|_{\mathbb{E}}$ for (7) with $\mu = 10^{-3}$, and rates of convergence (number of iterations)

ε	$N = 32$	$N = 64$	$N = 128$	$N = 256$	$N = 512$	$N = 1024$
1	4.08e-02	2.04e-02	1.02e-02	5.11e-03	2.55e-03	1.28e-03
	(2)	1.00 (2)	1.00 (2)	1.00 (2)	1.00 (2)	1.00 (2)
10^{-2}	1.08e-01	5.34e-02	2.65e-02	1.32e-02	6.61e-03	3.30e-03
	(3)	1.02 (3)	1.01 (2)	1.00 (2)	1.00 (2)	1.00 (2)
10^{-4}	5.44e-02	2.63e-02	1.31e-02	6.50e-03	3.24e-03	1.62e-03
	(6)	1.05 (3)	1.01 (3)	1.01 (2)	1.00 (2)	1.00 (2)
10^{-6}	2.27e-02	1.07e-02	5.30e-03	2.66e-03	1.33e-03	6.65e-04
	(8)	1.08 (3)	1.02 (3)	1.00 (2)	1.00 (2)	1.00 (2)
10^{-8}	1.82e-02	8.35e-03	4.10e-03	2.04e-03	1.02e-03	5.12e-04
	(9)	1.13 (4)	1.03 (3)	1.00 (2)	1.00 (2)	1.00 (2)
10^{-10}	1.80e-02	8.33e-03	4.07e-03	2.04e-03	1.02e-03	5.10e-04
	(9)	1.12 (4)	1.03 (3)	1.00 (3)	1.00 (3)	1.00 (2)
10^{-12}	1.80e-02	8.36e-03	4.08e-03	2.04e-03	1.02e-03	5.10e-04
	(9)	1.10 (5)	1.03 (3)	1.00 (3)	1.00 (3)	1.00 (3)

Since the results in a given column of Table 2 straddle multiple regimes, the robustness of the error estimates, with respect to the perturbation parameters, might not be so clear. Therefore, in

Table 3, we present results for a single value of N . Moreover, each row is restricted to a single case (as per Table 1) by taking a fixed value of μ , and only values of ε that correspond to the associated regime. For Cases (a) and (b), we see that the error is clearly robust with respect to ε , (suggesting the μ -weighted term in (8) dominates). For Case (c), the error scales as $\varepsilon^{1/4}$, as expected. We can conclude that the error bound (8) is satisfied.

Table 3: $\|E_h\|_E$ for $N = 1024$ for each case in Table 1

Case (a) $\mu = 1$	$\varepsilon = 10^{-4}$ 9.78e-03	$\varepsilon = 10^{-5}$ 9.73e-03	$\varepsilon = 10^{-6}$ 9.77e-03	$\varepsilon = 10^{-7}$ 9.78e-03	$\varepsilon = 10^{-8}$ 9.68e-03	$\varepsilon = 10^{-9}$ 9.68e-03	$\varepsilon = 10^{-10}$ 9.64e-03
Case (b) $\mu = 10^{-3}$	—	—	$\varepsilon = 10^{-8}$ 5.12e-04	$\varepsilon = 10^{-9}$ 5.10e-04	$\varepsilon = 10^{-10}$ 5.10e-04	$\varepsilon = 10^{-11}$ 5.10e-04	$\varepsilon = 10^{-12}$ 5.10e-04
Case (c) $\mu = 10^{-8}$	—	—	—	$\varepsilon = 10^{-6}$ 5.44e-04	$\varepsilon = 10^{-8}$ 1.71e-04	$\varepsilon = 10^{-10}$ 5.40e-05	$\varepsilon = 10^{-12}$ 1.70e-05

3 Two-dimensional problems

We now extend the approach presented in §2 to problems in two-dimensions. Again, at the core of the idea is the technique for generating layer-adapted meshes, of the Bakhvalov type, using MPDEs in (Hill and Madden, 2021), but now using iteratively computed derivative estimates to automatically detect the location and width of layers.

3.1 Two-dimensional SPDEs

We consider the family two-dimensional reaction-convection-diffusion equations of the form

$$-\varepsilon \Delta u(x, y) + \mu \mathbf{b} \cdot \nabla u(x, y) + u(x, y) = f(x, y),$$

$$\text{for } (x, y) \in \Omega := (0, 1)^2 \text{ and } u|_{\partial\Omega} = 0. \quad (9)$$

This motivates the two-dimensional MPDE formulation discussed in §3.2. In particular, the location and width of the layers in the solutions to (9) is dependent on the relative magnitude of ε and μ , as outlined for the one-dimensional problem in Table 1. However, there are two further complications: layers may occur at any of the four boundaries, and, depending on the direction of \mathbf{b} , boundary layers maybe exponential or parabolic in nature.

For a specific example, we consider the problem

$$-\varepsilon \Delta u(x, y) + \mu(3 - x)u_x + u(x, y) = e^{1+x+y},$$

$$\text{for } (x, y) \in \Omega := (0, 1)^2 \text{ and } u|_{\partial\Omega} = 0. \quad (10)$$

The possible variation in the solutions is demonstrated in Figure 2 which presents solutions to (9) for a selection of values for ε and μ . Note that the relative magnitude of ε and μ impacts the number of layers that are visible, their location, and their width.

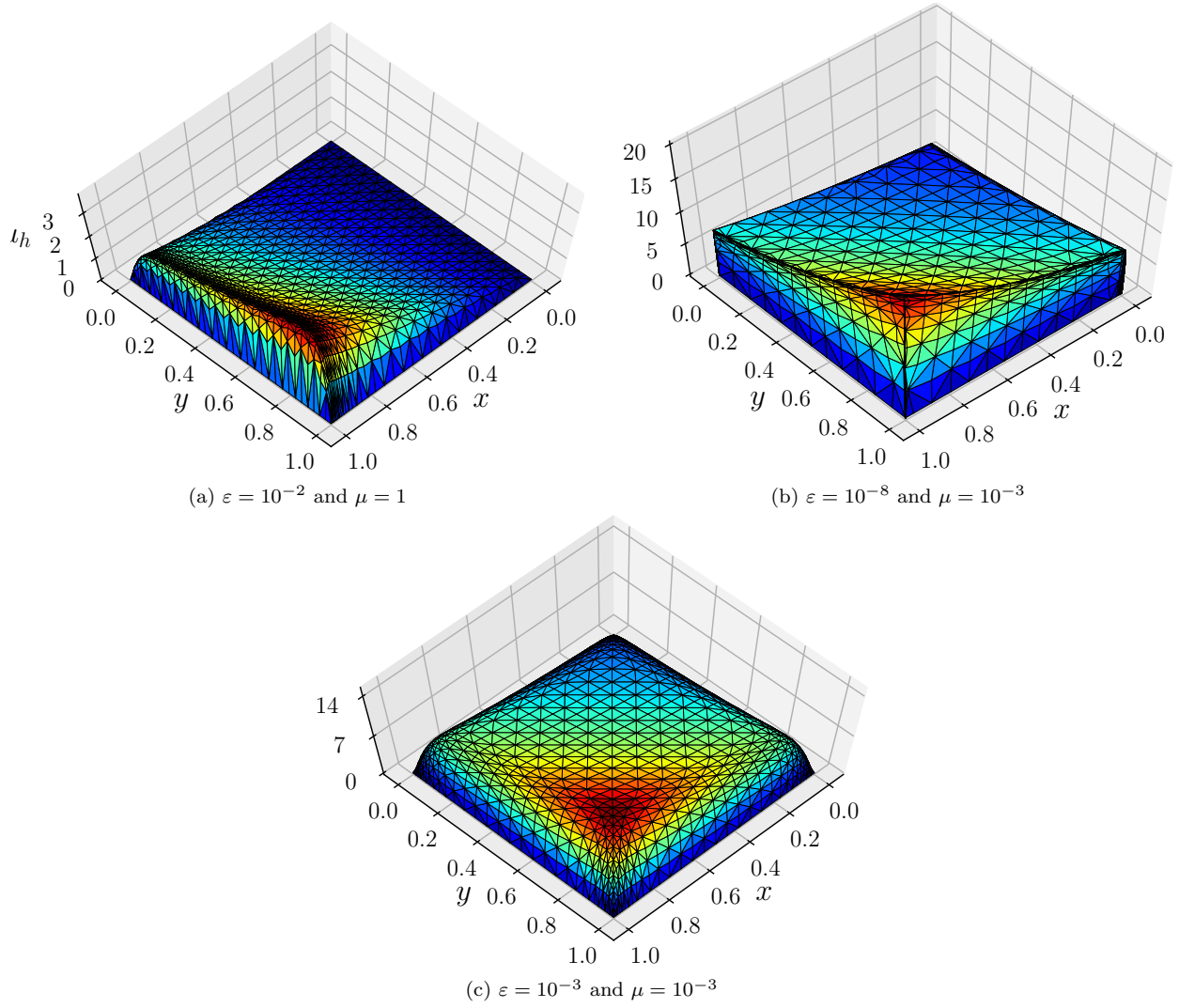
3.2 Two-dimensional MPDEs

For (9), a mesh that may be layer-adapted at any of the four boundaries is needed and so the MPDE is formulated as the two-dimension vector-valued Poisson equation, for $\mathbf{x}(\xi_1, \xi_2) = (x, y)^T$,

$$-\nabla^{[c]} \cdot (M(\mathbf{x}(\xi_1, \xi_2), u_h) \nabla^{[c]} \mathbf{x}(\xi_1, \xi_2)) = (0, 0)^T, \text{ for } (\xi_1, \xi_2) \in \Omega^{[c]}, \quad (11a)$$

subject to the boundary conditions

$$\begin{aligned} x(0, \xi_2) = 0, \quad x(1, \xi_2) = 1, \quad \frac{\partial x}{\partial \mathbf{n}}(\xi_1, 0) = 0, \quad \frac{\partial x}{\partial \mathbf{n}}(\xi_1, 1) = 0, \\ y(\xi_1, 0) = 0, \quad y(\xi_1, 1) = 1, \quad \frac{\partial y}{\partial \mathbf{n}}(0, \xi_2) = 0, \quad \frac{\partial y}{\partial \mathbf{n}}(1, \xi_2) = 0. \end{aligned} \quad (11b)$$

Figure 2: Examples of the FEM solution for (9) with $N = 32$

As before, the parameters K_1 and K_2 determine the proportion of mesh points in the layer regions, and σ is based on the formal order of them scheme.

The computational meshes that are to be computed are not necessarily tensor-product, however they are M -uniform. Therefore, we can denote the mesh points as $(x, y)_k$, for $k = 0, 1, \dots, (N+1)^2 - 1$, indexed using standard lexicographic ordering. For example, in Figure 3(b) we show the indices of the mesh points when $N = 4$.

In (11), we take

$$M(\mathbf{x}, u_h) = \begin{pmatrix} m_{1,1} & 0 \\ 0 & m_{2,2} \end{pmatrix}, \quad (12a)$$

where

$$\begin{aligned} m_{1,1}(\mathbf{x}, u_h) &= \max \left\{ 1, K_1 (v_4 \exp(-v_4 x \sigma^{-1}) + v_2 \exp(-v_2(1-x)\sigma^{-1})) \right\} \\ m_{2,2}(\mathbf{x}, u_h) &= \max \left\{ 1, K_2 (v_1 \exp(-v_1 y \sigma^{-1}) + v_3 \exp(-v_3(1-y)\sigma^{-1})) \right\}. \end{aligned} \quad (12b)$$

Here $m_{1,1}$ and $m_{2,2}$ can be thought of as extensions to the terms in (6) to two dimension: they encode that there may be layers adjacent the each of four boundaries. The terms v_1 , v_2 , v_3 and v_4 determine the magnitude and decay rate of the associated layer terms. Taken together, they relate to pointwise bounds on derivatives of $u(x, y)$ (Hill and Madden, 2021). Since each layer term decays rapidly away from its associated boundary, and takes its maximum at that boundary, the v_i terms are determined

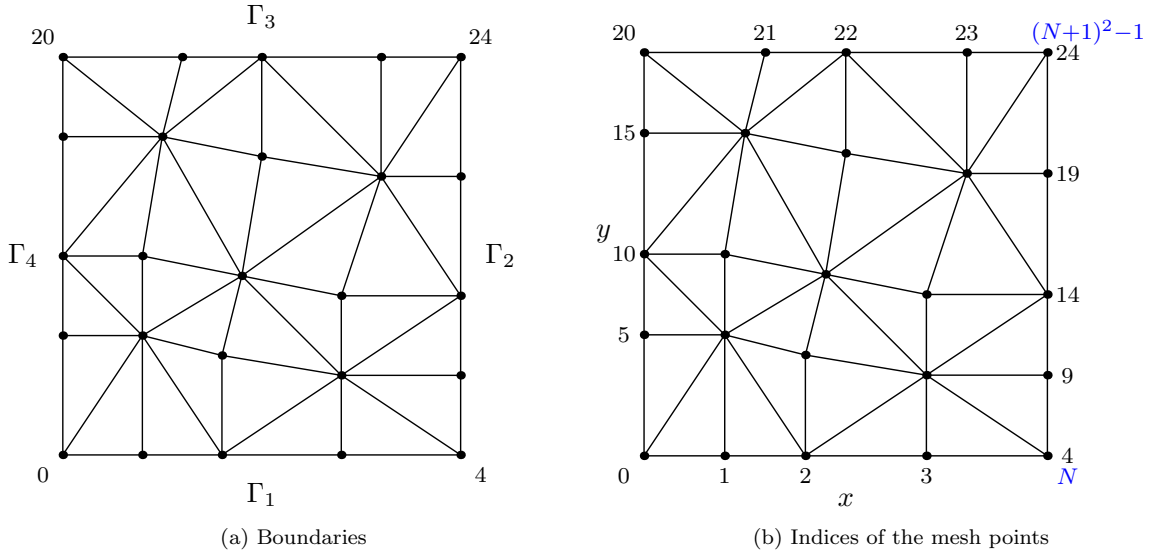


Figure 3: Example of boundaries and indices of mesh points on a non-tensor product grid with $N = 4$

by the appropriate derivatives of the numerical solution adjusted for the effects of the right-hand side of the SPDE, evaluated at the boundary. For efficiency, these are computed as

$$v_1(\mathbf{x}, u_h)_k = \frac{|(u_h)_{y^+}(x, y)_l|}{\max\{1, |f(x, y)_l|\}}, \text{ where } l = k \bmod N+1, \quad (13a)$$

$$v_2(\mathbf{x}, u_h)_k = \frac{|(u_h)_{x^-}(x, y)_l|}{\max\{1, |f(x, y)_l|\}}, \text{ where } l = N + \left\lfloor \frac{k}{N+1} \right\rfloor (N+1), \quad (13b)$$

$$v_3(\mathbf{x}, u_h)_k = \frac{|(u_h)_{y^-}(x, y)_l|}{\max\{1, |f(x, y)_l|\}}, \text{ where } l = N(N+1) + k \bmod N+1, \quad (13c)$$

$$v_4(\mathbf{x}, u_h)_k = \frac{|(u_h)_{x^+}(x, y)_l|}{\max\{1, |f(x, y)_l|\}}, \text{ where } l = \left\lfloor \frac{k}{N+1} \right\rfloor (N+1), \quad (13d)$$

where $k = 0, 1, \dots, (N+1)^2 - 1$, are the (lexicographic) indices of the mesh points, and $f(x, y)$ is the right-hand side of the SPDE. That is, these functions propagate the derivatives of u_h , adjusted by the value of $f(x, y)$ at their respective boundaries across the domain. For example, in the case where $N = 4$, we take $v_4(\mathbf{x}, u_h)$ to have the same value at each of the mesh points $k = 5, k = 6, \dots, k = 9$ (see Figure 3(b)), which is $|(u_h)_{x^+}(x, y)_5| / \max\{1, |f(x, y)_5|\}$. If one preferred, we could set, for example, $v_4(\mathbf{x}, u_h) = |(u_h)_{x^+}(0, y)| / \max\{1, |f(0, y)|\}$. However, we have verified that there is no noticeable advantage for the extra computational expense one would encounter on a non-tensor product grid.

Finally, we note that if a particular edge does not feature a layer the associate v_i term will be $\mathcal{O}(1)$, and so does not induce any refinement near that boundary.

3.3 Algorithm and implementation

Although the approach to numerically solving (11) efficiently is an extension of that used for the one-dimensional problem in §2.3, it has minor variations that merit further discussion. (For completeness the full algorithm is given in Appendix B). As in Algorithm 1, we take an initial mesh with $N = 16$. We then perform $\lceil 6 \log_{10}(\varepsilon^{-1}) \rceil$ iterations of the fixed-point method to resolve the MPDE sufficiently. Since only one mesh point is added to a layer region at each iteration, and we require the minimum mesh width to be $\mathcal{O}(\varepsilon/N)$, one can deduce that $\mathcal{O}(\log \varepsilon^{-1})$ iterations are required. Experiments indicate that $\lceil 6 \log_{10} \varepsilon^{-1} \rceil$ iterations suffice.

We then alternate between a sequence of uniform h -refinements of the computational mesh, and 5 iterations of the fixed point method for the MPDE on each of these, until the mesh has the required number of mesh points.

Computational experimentation indicated that this approach is sufficient, and more efficient than iterating until a specified tolerance is achieved.

3.4 Numerical results

The mesh for (10) is generated using Algorithm 2 with MPDE (11). We set $K_1 = K_2 = 0.28$ which results in approximately 30% of the mesh points being located in each layer region. One takes $\sigma > p+1$, where p is the order of the FEM, so we have set $\sigma = 2.5$ for this \mathcal{P}_1 -FEM.

An example of the mesh for (10) generated using (11) is shown in Figure 4 and one observes that this is not a tensor-product grid. In Figure 5(b), one sees that the layer regions in the related SPDE are resolved when transformed onto the computational domain, $\Omega^{[c]}$.

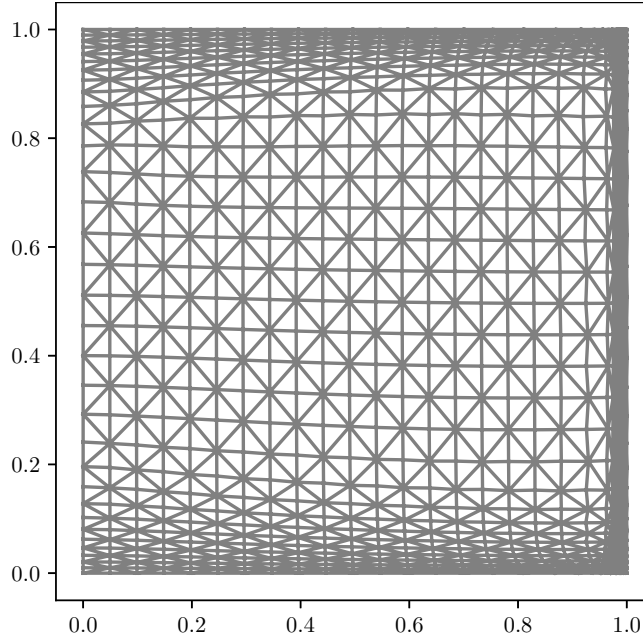


Figure 4: Mesh for (10) with $N = 32$, $\varepsilon = 10^{-3}$ and $\mu = 10^{-1}$

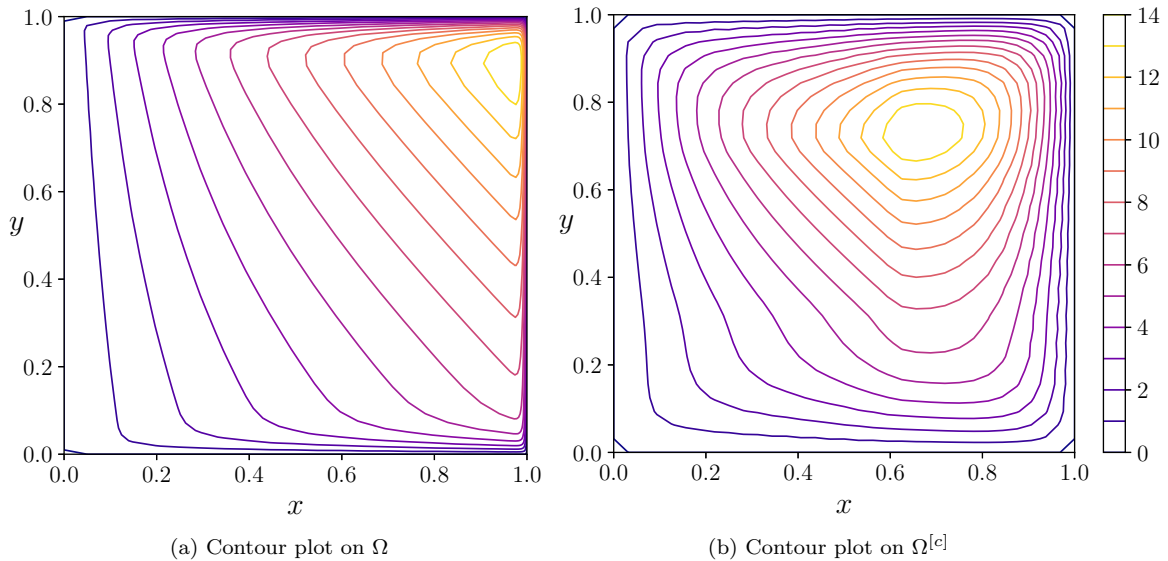


Figure 5: Contour plots with $N = 32$, $\varepsilon = 10^{-3}$, and $\mu = 10^{-1}$

As in §2.4, we first fix $\mu = 10^{-3}$, and take various values for ε , so that each of the three regimes is represented. The errors measured in the energy norm for (10) when solved on a mesh generated using Algorithm 2 are shown in Table 4. These clearly show that results are robust with respect to ε , and first-order convergent with respect to N

Table 4: $\|E_h\|_{\mathbb{E}}$ for (10) solved on meshes generated using Algorithm 2, with $\mu = 10^{-3}$, and various values of N and ε

ε/N	32	64	128	256	512
1	8.19e-02	4.10e-02	2.05e-02	1.03e-02	5.13e-03
		1.00	1.00	1.00	1.00
10^{-2}	2.79e-01	1.38e-01	6.83e-02	3.40e-02	1.69e-02
		1.02	1.01	1.01	1.00
10^{-4}	1.22e-01	5.97e-02	2.96e-02	1.47e-02	7.34e-03
		1.03	1.01	1.01	1.00
10^{-6}	5.14e-02	2.49e-02	1.23e-02	6.13e-03	3.06e-03
		1.05	1.01	1.01	1.00
10^{-8}	4.03e-02	1.94e-02	9.66e-03	4.80e-03	2.39e-03
		1.05	1.01	1.01	1.01
10^{-10}	3.92e-02	1.90e-02	9.45e-03	4.70e-03	2.34e-03
		1.04	1.01	1.01	1.00
10^{-12}	3.91e-02	1.90e-02	9.44e-03	4.69e-03	2.34e-03
		1.04	1.01	1.01	1.01

In Table 5, we fix $N = 512$, and examine the results for various values of ε and μ . Again, we see robust convergence with ε in each different regime. It should be noted that, for $\mu = 1$ and $\mu = 10^{-3}$, the problem is essentially convection-dominated, and so there is no ε dependency in the computed errors. For $\mu = 10^{-8}$, the problem is dominated by the reaction term, and so the ε -dependency in the error is consistent with (8), and with those shown in Table 3 for the one-dimensional problem. /

Table 5: $\|E_h\|_{\mathbb{E}}$ for (10) with $N = 512$ for each case in Table 1

Case (a)	$\varepsilon = 10^{-4}$	$\varepsilon = 10^{-5}$	$\varepsilon = 10^{-6}$	$\varepsilon = 10^{-7}$	$\varepsilon = 10^{-8}$	$\varepsilon = 10^{-9}$	$\varepsilon = 10^{-10}$
$\mu = 1$	3.90e-02	3.49e-02	3.40e-02	3.39e-02	3.28e-02	3.46e-02	3.29e-02
Case (b)			$\varepsilon = 10^{-8}$	$\varepsilon = 10^{-9}$	$\varepsilon = 10^{-10}$	$\varepsilon = 10^{-11}$	$\varepsilon = 10^{-12}$
$\mu = 10^{-3}$			2.39e-03	2.35e-03	2.34e-03	2.34e-03	2.34e-03
Case (c)				$\varepsilon = 10^{-6}$	$\varepsilon = 10^{-8}$	$\varepsilon = 10^{-10}$	$\varepsilon = 10^{-12}$
$\mu = 10^{-8}$				2.44e-03	7.84e-04	2.49e-04	7.91e-05

4 Conclusions and future work

The MPDEs presented in (5) and (11) use *a posteriori* information about the related SPDE. More precisely, using only the knowledge that the solution possesses boundary layers (but not their location or width) layer-adapted meshes are generated. The solutions are robust and the errors converge as expected. The magnitude and rates of convergence of the errors are similar to when the solutions are generated using the MPDE method based on *a priori* information (Hill and Madden, 2021). Our investigations included ensuring that the local mesh width is appropriate for the relevant layer width, though, for brevity, we have not included the detail.

There are numerous possibilities for extending this work. Perhaps the most obvious, and challenging, is to generalise the approach to produce layer-adapted meshes for interior layer problems. Work in this direction is currently in its infancy.

Acknowledgement: The work of RH is supported by the Irish Research Council, GOIPG/2017/463 & GOIPD/2022/284.

Appendices

A FEniCS code to compute a 1D layer-adapted mesh

Here we present Python code an implementation of Algorithm 1 for solving

$$-\varepsilon u''(x) + \mu b(x)u'(x) + r(x)u(x) = f(x) \quad \text{for } x \in (0,1), \quad \text{and } u(0) = u(1) = 0,$$

for the specific example in (7) with $\varepsilon = 10^{-3}$, $\mu = 10^{-3}$ and $N = 32$. We use the Gauss Lobatto quadrature rule to solve both the MPDE and SPDE. (See the note in (Hill and Madden, 2021, App. B) for why this is necessary).

```

## 1DMPDE_dx_RCD_code.py
# FEniCS version: 2019.2.0.dev0
# Generate a layer-adapted mesh for the one-dimensional
# reaction-convection-diffusion equation
# -eps u'' + mu u' + u = exp(1+x) for x in (0,1) with u(0)=u(1)=0,
# via mesh partial differential equations and a posteriori information using
# -(rho(x) x'(xi))' = 0 for xi in (0,1) with x(0) = x(1) = 1.
from fenics import *
import math; import numpy as np
# Change quadrature rule to Gauss Lobatto
from FIAT.reference_element import *
from FIAT.quadrature import *
from FIAT.quadrature_schemes import create_quadrature
def create_GaussLobatto_quadrature(ref_el, degree, scheme="default"):
    if degree < 3: degree = 3
    return GaussLobattoLegendreQuadratureLineRule(ref_el, degree)
import FIAT
FIAT.create_quadrature = create_GaussLobatto_quadrature

# Parameters for physical problem and mesh size
epsilon = 1.0e-3 # coefficient of diffusion term
mu = 1.0e-3 # coefficient of convection term
f = Expression('exp(1.0+x[0])', degree=2) # RHS of SPDE
N = 2**5 # Max mesh intervals; at least 2**4

# Parameters for MPDE
K = 0.28 # proportion of mesh points in layers
sigma = 2.5 # related to degree of elements
x_init = Expression('x[0]', degree=2) # Initial solution to the MPDE

# Parameters for stepping through N
N_start = 2**4 # initial mesh size
TOL = 1.0e-3 # Stopping criterion tolerance

# Lists to store meshes and function spaces (as we step through mesh sizes)
meshc_list, mesh_list = [None]*int(math.log(N,2)-3), []
Vc_list, V_list = [None]*int(math.log(N,2)-3), []

def comp_space(N): # Computational function space parameters
    meshc = UnitIntervalMesh(N)
    Vc = FunctionSpace(meshc, 'P', 1) # Function space with P1-elements
    vc = TestFunction(Vc) # Test function on Vc
    xc = TrialFunction(Vc) # Trial function on Vc
    return meshc, Vc, vc, xc

def MPDE_FEM(rho, x_old, u_h_x0, u_h_xN, xc, vc, meshc, Vc): # Solve MPDE
    bc = DirichletBC(Vc, x_init, 'on_boundary')
    a = rho(x_old, u_h_x0, u_h_xN)*inner(grad(xc), grad(vc))*dx(meshc) # LHS of MPDE
    L = Constant("0.0")*vc*dx # MPDE is homogeneous
    x_new = Function(Vc) # New mesh function
    solve(a==L, x_new, bc)
    return x_new

def rho(x, u_h_x0, u_h_xN): # Define rho(x) for MPDE
    upsilon_0 = u_h_x0/max(1.0,f(0.0))
    upsilon_1 = u_h_xN/max(1.0,f(1.0))
    return conditional((K*(upsilon_0*exp(-upsilon_0*x/sigma)+upsilon_1*exp(-upsilon_1*(1-x)/sigma))>1.0,\
        (K*(upsilon_0*exp(-upsilon_0*x/sigma)+upsilon_1*exp(-upsilon_1*(1-x)/sigma))), 1.0)

def phys_space(N, x): # Physical function space parameters

```

```

mesh = UnitIntervalMesh(N)
mesh.coordinates()[:,0] = x.compute_vertex_values()[:]
V = FunctionSpace(mesh, 'P', 1)          # Function space with P1-elements
v = TestFunction(V)                    # Test function on V
u = TrialFunction(V)                    # Trial function on V
return mesh, V, v, u

def SPDE_FEM(u, v, mesh, V): # Solve reaction-convection-diffusion problem
    bcp = DirichletBC(V, "0.0", 'on_boundary')
    a = epsilon*dot(grad(u), grad(v))*dx(mesh) \
        + mu*u.dx(0)*v*dx + u*v*dx
    L = f*v*dx
    u_h = Function(V)
    solve(a==L, u_h, bcp)
    # calculate the derivatives of u_h on the first and last intervals
    u_h_x = (project(u_h.dx(0), V)).compute_vertex_values()
    u_h_x0, u_h_xN = abs(u_h_x[0]), abs(u_h_x[-1])
    return u_h, u_h_x0, u_h_xN

# Initial values
u_h_x0, u_h_xN = 1.0, 1.0
meshc_list[0], Vc_list[0], vc, xc = comp_space(N_start)
x = interpolate(x_init, Vc_list[0])     # Initial value for x

k = 0
for i in range(0, int(math.log(N,2)-3)): # Iterate through h-refinements
    N_step = 2**(i+4)                    # mesh size
    Delta = TOL+1
    while Delta > TOL:
        mesh_list.append(None), V_list.append(None)
        mesh_list[k], V_list[k], v, u = phys_space(N_step, x)
        u_h_x0_old, u_h_xN_old = u_h_x0, u_h_xN
        u_h, u_h_x0, u_h_xN = SPDE_FEM(u, v, mesh_list[k], V_list[k])
        Delta = abs((u_h_x0-u_h_x0_old)/u_h_x0)+abs((u_h_xN-u_h_xN_old)/u_h_xN)
        x = MPDE_FEM(rho, x, u_h_x0, u_h_xN, xc, vc, meshc_list[i], Vc_list[i])
        k = k+1
    if N_step < N:
        # Generate computational function space on the finer mesh
        meshc_list[i+1], Vc_list[i+1], vc, xc = comp_space(N_step*2)
        # Interpolate the solution onto the new computational function space
        x = interpolate(x, Vc_list[i+1])
        # Generate physical function space on the finer mesh
        mesh_list[i+1], V_list[i+1], v, u = phys_space(N_step*2, x)

# final (adapted) mesh and solution to SPDE
mesh_list.append(None), V_list.append(None)
mesh_list[k], V_list[k], v, u = phys_space(N, x)
u_h, u_h_x0, u_h_xN = SPDE_FEM(u, v, mesh_list[k], V_list[k])

```

B 2D Algorithm

Inputs: N , the number of intervals in both directions in the final mesh on $\Omega^{[c]}$; M , a mesh density function.

- 1 Set $\omega_h^{[c;0]} := \{(\xi_1, \xi_2)_i\}_{i=0}^{16}$ to be a uniform tensor-product mesh on $\bar{\Omega}^{[c]}$ with 16 mesh intervals in each coordinate direction;
- 2 Set $\mathbf{x}(\xi_1, \xi_2) = (\xi_1, \xi_2)$ for $(\xi_1, \xi_2) \in \bar{\Omega}^{[c]}$;
- 3 $\mathbf{r} \leftarrow \mathbf{x}$; $k \leftarrow 0$;
- 4 **for** j in $0 : \lceil 6 \log_{10}(\varepsilon^{-1}) \rceil$ **do**
 - 5 Set $\omega_h^{[k]} := \mathbf{x}(\omega_h^{[c;0]})$ to be the adapted mesh on $\bar{\Omega}$ at step k ;
 - 6 $u_h^{[k]} \leftarrow \mathcal{P}_1$ -FEM solution to the SPDE on $\omega_h^{[k]}$;
 - 7 Calculate $v_l^{[k]}(\mathbf{r}, u_h^{[k]})$ for $l = 1, 2, 3, 4$, and then $M(\mathbf{r}, u_h^{[k]})$, as in (12);
 - 8 Set \mathbf{x} to be the \mathcal{P}_1 -FEM solution, on $\omega_h^{[c;0]}$, to

$$\nabla \cdot (M(\mathbf{r}, u_h^{[k]}) \nabla \mathbf{x}(\xi_1, \xi_2)) = (0, 0)^T, \text{ for } (\xi_1, \xi_2) \in \Omega^{[c]}, \quad (14)$$
 with boundary conditions as defined in (11b);
 - 9 $\mathbf{r} \leftarrow \mathbf{x}$; $k \leftarrow k+1$;
- 10 **end**
- 11 **for** i in $1 : (\log_2(N) - 4)$ **do**
 - 12 $w^{[c;i]} \leftarrow$ uniform h -refinement of $w^{[c;i-1]}$;
 - 13 $\mathbf{r} \leftarrow \mathbf{r}$ interpolated onto $w^{[c;i]}$;
 - 14 **for** j in $1 : 4$ **do**
 - 15 Set $\omega_h^{[k]} := \mathbf{x}(\omega_h^{[c;i]})$ to be the adapted mesh on $\bar{\Omega}$ at step k ;
 - 16 $u_h^{[k]} \leftarrow \mathcal{P}_1$ -FEM solution to the SPDE on $\omega_h^{[k]}$;
 - 17 Calculate $v_l^{[k]}(\mathbf{r}, u_h^{[k]})$ for $l = 1, 2, 3, 4$ and then $M(\mathbf{r}, u_h^{[k]})$, as in (12);
 - 18 Set \mathbf{x} to be the \mathcal{P}_1 -FEM solution, on $\omega_h^{[c;i]}$, to

$$\nabla \cdot (M(\mathbf{r}, u_h^{[k]}) \nabla \mathbf{x}(\xi_1, \xi_2)) = (0, 0)^T, \text{ for } (\xi_1, \xi_2) \in \Omega^{[c]}, \quad (15)$$
 with boundary conditions as defined in (11b);
 - 19 $\mathbf{r} \leftarrow \mathbf{x}$; $k \leftarrow k+1$;
 - 20 **end**
- 21 **end**
- 22 Set $\omega_h := \mathbf{x}(\omega_h^{[c;i]})$ to be the adapted mesh on $\bar{\Omega}$;

Algorithm 2: Generate a two-dimensional layer-adapted mesh using an MPDE using *a posteriori* information and h -refinement.

References

- Bakhvalov, N.S., 1969. On the optimization of the methods for solving boundary value problems in the presence of a boundary layer. *Ž. Vyčisl. Mat i Mat. Fiz.* 9, 841–859.
- Beckett, G., Mackenzie, J.A., 2000. Convergence analysis of finite difference approximations on equidistributed grids to a singularly perturbed boundary value problem. *Appl. Numer. Math.* 35, 87–109. doi:10.1016/S0168-9274(99)00065-3.
- Brdar, M., Zarin, H., 2016. A singularly perturbed problem with two parameters on a Bakhvalov-type mesh. *J. Comput. Appl. Math.* 292, 307–319. doi:10.1016/j.cam.2015.07.011.
- Gracia, J.L., O’Riordan, E., Pickett, M.L., 2006. A parameter robust second order numerical method

- for a singularly perturbed two-parameter problem. *Appl. Numer. Math.* 56, 962–980. doi:10.1016/j.apnum.2005.08.002.
- Hill, R., Madden, N., 2021. Generating layer-adapted meshes using mesh partial differential equations. *Numer. Math. Theory Methods Appl.* 14, 559–588. doi:10.4208/nmtma.oa-2020-0187.
- Kopteva, N., Stynes, M., 2001. A robust adaptive method for a quasi-linear one-dimensional convection-diffusion problem. *SIAM J. Numer. Anal.* 39, 1446–1467. doi:10.1137/S003614290138471X.
- Linß, T., 2010. Layer-Adapted Meshes for Reaction-Convection-Diffusion Problems. volume 1985 of *Lecture Notes in Mathematics*. Springer-Verlag, Berlin. doi:10.1007/978-3-642-05134-0.
- Logg, A., Mardal, K.A., Wells, G.N. (Eds.), 2012. Automated Solution of Differential Equations by the Finite Element Method. volume 84 of *Lecture Notes in Computational Science and Engineering*. Springer, Heidelberg. doi:10.1007/978-3-642-23099-8. the FEniCS book.
- Miller, J.J.H., O’Riordan, E., Shishkin, G.I., 2012. Fitted Numerical Methods for Singular Perturbation Problems. Revised ed., World Scientific Publishing Co. Pte. Ltd., Hackensack, NJ. doi:10.1142/9789814390743. error estimates in the maximum norm for linear problems in one and two dimensions.
- O’Malley, Jr., R.E., 1967. Two-parameter singular perturbation problems for second-order equations. *J. Math. Mech.* 16, 1143–1164.
- Roos, H.G., 2022. Robust numerical methods for singularly perturbed differential equations—supplements. <https://arxiv.org/abs/2209.02994>. doi:10.48550/arXiv.2209.02994, arXiv:2209.02994.
- Roos, H.G., Stynes, M., Tobiska, L., 2008. Robust Numerical Methods for Singularly Perturbed Differential Equations. volume 24 of *Springer Series in Computational Mathematics*. Second ed., Springer-Verlag, Berlin. Convection-Diffusion-Reaction and Flow Problems.
- Roos, H.G., Uzelac, Z., 2003. The SDFEM for a convection-diffusion problem with two small parameters. *Comput. Methods Appl. Math.* 3, 443–458. doi:10.2478/cmam-2003-0029.
- Shakti, D., Mohapatra, J., Das, P., Vigo-Aguiar, J., 2022. A moving mesh refinement based optimal accurate uniformly convergent computational method for a parabolic system of boundary layer originated reaction-diffusion problems with arbitrary small diffusion terms. *J. Comput. Appl. Math.* 404, Paper No. 113167, 16. doi:10.1016/j.cam.2020.113167.
- Shishkin, G.I., Shishkina, L.P., 2009. Difference Methods for Singular Perturbation Problems. volume 140 of *Chapman & Hall/CRC Monographs and Surveys in Pure and Applied Mathematics*. CRC Press, Boca Raton, FL.
- Sikwila, S.T., Shateyi, S., 2013. A moving mesh method for singularly perturbed problems. *Abstr. Appl. Anal.*, Art. ID 214505, 11doi:10.1155/2013/214505.
- Singh, G., Natesan, S., 2020. Study of the NIPG method for two-parameter singular perturbation problems on several layer adapted grids. *J. Appl. Math. Comput.* 63, 683–705. doi:10.1007/s12190-020-01334-7.
- Wu, Y., Zhang, N., Yuan, J., 2013. A robust adaptive method for singularly perturbed convection-diffusion problem with two small parameters. *Comput. Math. Appl.* 66, 996–1009. doi:10.1016/j.camwa.2013.06.025.
- Zhang, J., Lv, Y., 2022. Supercloseness of finite element method on a Bakhvalov-type mesh for a singularly perturbed problem with two parameters. *Appl. Numer. Math.* 171, 329–352. doi:10.1016/j.apnum.2021.09.010.